Supplemental Document

Optics EXPRESS

Parity-pair-mixing effects in nonlinear spectroscopy of HDO: supplement

MEISSA L. DIOUF,[1] ROLAND TÓBIÁS,[2] FRANK M. J. COZIJN,[1] EDCEL J. SALUMBIDES,[1] CSABA FÁBRI,[2] CRISTINA PUZZARINI,[3] ATTILA G. CSÁSZÁR,[2,4] AND WIM UBACHS[1,*]

[1] *Department of Physics and Astronomy, LaserLaB, Vrije Universiteit, De Boelelaan 1081, 1081 HV Amsterdam, The Netherlands*
[2] *Laboratory of Molecular Structure and Dynamics, Institute of Chemistry, ELTE Eötvös Loránd University and MTA-ELTE Complex Chemical Systems Research Group, H-1117 Budapest, Pázmány Péter sétány 1/A, Hungary*
[3] *Dipartimento di Chimica "Giacomo Ciamician", Universitá di Bologna, Via F. Selmi 2, I-40126 Bologna, Italy*
[4] *attila.csaszar@ttk.elte.hu*
[*] *w.m.g.ubachs@vu.nl*

Supplement DOI: https://doi.org/10.6084/m9.figshare.21520698

Parent Article DOI: https://doi.org/10.1364/OE.474525

Parity-pair-mixing effects in nonlinear spectroscopy of HDO

MEISSA L. DIOUF,[1] ROLAND TÓBIÁS,[2] FRANK M. J. COZIJN,[1] EDCEL J. SALUMBIDES,[1] CSABA FÁBRI,[2] CRISTINA PUZZARINI,[3] ATTILA G. CSÁSZÁR,[2,*] AND WIM UBACHS[1,*]

[1] *Department of Physics and Astronomy, LaserLaB, Vrije Universiteit, De Boelelaan 1081, 1081 HV Amsterdam, The Netherlands*
[2] *Laboratory of Molecular Structure and Dynamics, Institute of Chemistry, ELTE Eötvös Loránd University and MTA-ELTE Complex Chemical Systems Research Group, H-1117 Budapest, Pázmány Péter sétány 1/A, Hungary*
[3] *Dipartimento di Chimica "Giacomo Ciamician," Universitá di Bologna, Via F. Selmi 2, I-40126 Bologna, Italy*
[*] *w.m.g.ubachs@vu.nl, attila.csaszar@ttk.elte.hu*

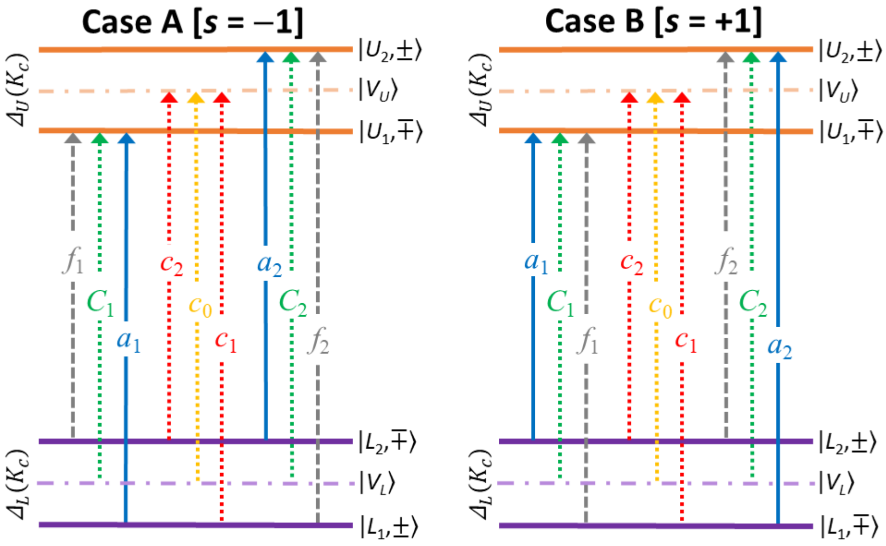

Figure S1. Two cases of the nonuplet model utilized in this study. The symbols of this figure are defined in the caption to Fig. 7 (see the main text). The only exception, s, is specified as +1 (–1) if the parities of L_1 and U_1 are identical (different). Cases A and B correspond to those cases when $s = -1$ and $s = +1$, respectively. Note that $L_2 \leftarrow L_1$ and $U_2 \leftarrow U_1$ are also dipole-allowed (a-type) transitions, but they are far off-resonant with our laser frequency and thus not displayed.

S1. Expressions for the relative positions of lines in Fig. S1

Upon a close look at Fig. S1, a set of constraints can be formulated among the nine resonance frequencies by using the principle of combination differences. Neglecting "(K_c)" from the symbols of the two K_c splittings to improve readability, one can deduce the following equations valid for the two cases shown on Fig. S1:

$$C_i = c_0 + (-1)^i \Delta_U/2, \tag{S1}$$

$$c_i = c_0 + (-1)^{i+1} \Delta_L/2, \tag{S2}$$

$$a_i = C_i + (-1)^i s\Delta_L/2 = c_0 + (-1)^i \left[\Delta_U + s\Delta_L\right]/2, \tag{S3}$$

$$f_i = a_{3-i} + (-1)^i \Delta_U = c_0 + (-1)^i \left[\Delta_U - s\Delta_L\right]/2, \tag{S4}$$

where $X \in \{L, U\}$, $i \in \{1, 2\}$, and s is +1 or −1, depending on whether L_1 and U_1 have identical or opposite parity, respectively. In Eqs. (S3) and (S4), the expressions for C_i and a_i, respectively, are taken into account. It is clear from Eqs. (S1)–(S4) that the resonance frequencies C_i, c_i, a_i, and f_i can be calculated from the two splittings and the c_0 frequency. Furthermore, the expressions

$$\Delta C_i \equiv C_i - c_0 = (-1)^i \Delta_U/2, \tag{S5}$$

$$\Delta c_i \equiv c_i - c_0 = (-1)^{i+1} \Delta_L/2, \tag{S6}$$

$$\Delta a_i \equiv a_i - c_0 = (-1)^i \left[\Delta_U + s\Delta_L\right]/2, \tag{S7}$$

$$\Delta f_i \equiv f_i - c_0 = (-1)^i \left[\Delta_U - s\Delta_L\right]/2, \tag{S8}$$

imply that the frequencies relative to c_0 depend only on the splittings Δ_L and Δ_U. The possible frequency orderings of the nonuplet lines are collected in Table S1.

Table S1. All possible frequency orderings of the nonuplet lines defined in Fig. S1.[a]

Case	Subcase	Frequency ordering
$s=-1$ [Case A]	$\Delta_L > 2\Delta_U$	$f_1 \le c_2 \le a_2 < C_1 \le c_0 \le C_2 < a_1 \le c_1 \le f_2$
	$2\Delta_U > \Delta_L \ge \Delta_U$	$f_1 \le c_2 \le C_1 \le a_2 \le c_0 \le a_1 \le C_2 \le c_1 \le f_2$
	$\Delta_U > \Delta_L \ge \Delta_U/2$	$f_1 < C_1 < c_2 < a_1 < c_0 < a_2 < c_1 < C_2 < f_2$
	$\Delta_U/2 > \Delta_L$	$f_1 \le C_1 \le a_1 < c_2 \le c_0 \le c_1 < a_2 \le C_2 \le f_2$
$s=1$ [Case B]	$\Delta_L > 2\Delta_U$	$a_1 \le c_2 \le f_2 < C_1 \le c_0 \le C_2 < f_1 \le c_1 \le a_2$
	$2\Delta_U > \Delta_L \ge \Delta_U$	$a_1 \le c_2 \le C_1 \le f_2 \le c_0 \le f_1 \le C_2 \le c_1 \le a_2$
	$\Delta_U > \Delta_L \ge \Delta_U/2$	$a_1 < C_1 < c_2 < f_1 < c_0 < f_2 < c_1 < C_2 < a_2$
	$\Delta_U/2 > \Delta_L$	$a_1 \le C_1 \le f_1 < c_2 \le c_0 \le c_1 < f_2 \le C_2 \le a_2$

[a] The symbols of this table are specified in the caption to Fig. 7 (see the main text) and Fig. S1. Cases A and B (see the first column) correspond to the two cases of Fig. S1. The second column contains the subcases, that is the relations between Δ_U and Δ_L, where Δ_X is an abbreviated form of the $\Delta_X(K_c)$ splitting. The third column provides the frequency orderings related to the individual (case,subcase) pairs.

S2. Resonances around the $(0\,0\,2)3_{2,1/2} \leftarrow (0\,0\,0)3_{3,0/1}$ doublet

Figure S2 exhibits the resonances around the $(0\,0\,2)3_{2,1/2} \leftarrow (0\,0\,0)3_{3,0/1}$ doublet of $HD^{16}O$. First, only the a-type lines, a_1 and a_2, were probed, for which fully symmetric Lamb dips were obtained. Nevertheless, a significant deviation, 91 kHz, was found for the $(0\,0\,0)3_{3,0/1}$ splitting, whose experimental value relies on a_1 and a_2. Assuming that this large deviation is caused by parity-pair mixing, an attempt was made to identify the f-type analogues of a_1 and a_2, as well. Despite their low intensity, which is due to the relatively high, but still sub-GHz-level $(0\,0\,0)3_{3,0/1}$ splitting, these f-type lines, f_1 and f_2, were indeed measurable *via* a 30-hour averaging of multiple scans [see panels (c) and (d)]. Although the appearance of further resonances at the sides of f_1 and f_2 is less clear for the moment, the results of Fig. S2 corroborate our assumption that the frequency shifts of a_1 and a_2 are associated with the AC-Stark interaction of the $(0\,0\,0)3_{3,0/1}$ pair. The cross-over resonances, missing from the energy-level scheme of Fig. S2, are not investigated in this study.

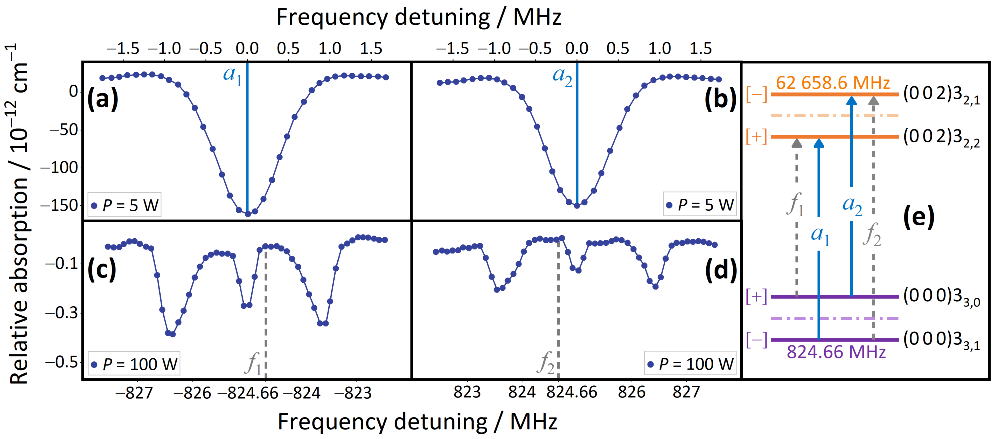

Figure S2. Four resonances involving the $(0\,0\,2)3_{2,1/2}$ and $(0\,0\,0)3_{3,0/1}$ parity pairs of $HD^{16}O$. The line centers, corresponding to zero detunings, are at 214 771 692 247 kHz [panel (a)] and 214 833 573 271 kHz [panel (b)]. Panels (a)–(b) and (c)–(d) exhibit dipole-allowed (a-type) and dipole-forbidden (f-type) transitions, respectively. The f_1 and f_2 resonances are offset by ∓824.66 MHz from a_1 and a_2, respectively [see also panel (e)]. P = intra-cavity power.